Journal of Hydrology 570 (2019) 80–95

Contents lists available at ScienceDirect

Journal of Hydrology

journal homepage: www.elsevier.com/locate/jhydrol

Research papers

Understanding the role of regional water connectivity in mitigating climate change impacts on surface water supply stress in the United States

Kai Duan[a,b,c,*], Peter V. Caldwell[c], Ge Sun[d], Steven G. McNulty[d], Yang Zhang[e], Erik Shuster[f], Bingjun Liu[a], Paul V. Bolstad[b]

[a] School of Civil Engineering, Sun Yat-Sen University, Guangzhou, China
[b] Department of Forest Resources, University of Minnesota, Saint Paul, MN, USA
[c] Coweeta Hydrologic Laboratory, USDA Forest Service, Otto, NC, USA
[d] Eastern Forest Environmental Threat Assessment Center, USDA Forest Service, Research Triangle Park, NC, USA
[e] Department of Marine, Earth, and Atmospheric Sciences, North Carolina State University, Raleigh, NC, USA
[f] National Energy Technology Laboratory, US Department of Energy, Pittsburgh, PA, USA

ARTICLE INFO

This manuscript was handled by C. Corradini, Editor-in-Chief, with the assistance of Weiping Chen, Associate Editor

Keywords:
Water stress
Water connectivity
Climate change
Upstream flow
Water transfer
Water consumption

ABSTRACT

Surface water supply for a watershed relies on local water generated from precipitation and water connections with other watersheds. These connections are confined by topography and infrastructure, and respond diversely to stressors such as climate change, population growth, increasing energy and water demands. This study presents an integrative simulation and evaluation framework that incorporates the natural and anthropogenic water connections (i.e., stream flows, inter-basin water transfers, water withdrawals and return flows) among the 2099 8-digit Hydrologic Unit Code (HUC-8) watersheds across the conterminous United States. The framework is then applied to investigate the potential impacts of changes in climate and water use on regional water availability and water stress (the ratio of demand to supply). Our projections suggest that highly water-stressed areas may expand from 14% to 18% and the stressed population would increase from 19% to 24% by 2070–2099. Climate-change mitigation practices (e.g., energy structure reform, technology innovation) could largely offset these trends by reducing demand and enhancing supply. At the watershed scale, the spatially inhomogeneous responses to future changes suggest that regional water connectivity could significantly buffer the potential stress escalations due to the redistribution of water resources and diverse changes in consumptive uses and water supplies in different source areas. However, the detrimental future changes (e.g., depleting river discharges, larger demands of water withdrawal) may aggravate conflicts over water rights among regions and challenge our current water infrastructure system. This study provides new insights into the critical role of regional water connectivity in water supply security, and highlights the increasing need for integrated monitoring and management of water resources at various spatial levels in a changing world.

1. Introduction

Changing environments and growing populations have stressed water resources both globally and in the United States (Foti et al., 2012; Kiguchi et al., 2015; Scherer et al., 2015). A measure commonly used to quantify water stress is the ratio of water demand (i.e., offstream water use) to water supply (i.e., water resources available to humans) (Richey et al., 2015; Sun et al., 2008). Water stress is constantly changing with environmental and anthropogenic dynamics such as the changes in population (Vörösmarty et al., 2000), economy and energy structure (Moore et al., 2015), water use efficiency (Maupin et al., 2014), and magnitude and variability of river discharges (Sagarika et al., 2014). Climate change poses an additional threat to water resources security. There is evidence that the warming climate enhances evapotranspiration (ET), and causes surface drying and subsequent depletion in water storage on the surface of the earth (Duan et al., 2016; Jackson et al., 2005). Water demand, on the other hand, could also be sensitive to climate change and the associated changes in environment, such as the rising temperature (Sailor and Pavlova, 2003), increasing CO_2 concentration (Elliott et al., 2014), and intensified drought (Döll et al., 2015; Sun et al., 2015a). It is becoming increasingly important to assess the vulnerability of water supply to global change so that management strategies can be developed to cope with a highly uncertain future (Alcamo et al., 2000; IPCC, 2014).

* Corresponding author at: School of Civil Engineering, Sun Yat-Sen University, Guangzhou, China.
E-mail address: duank6@mail.sysu.edu.cn (K. Duan).

https://doi.org/10.1016/j.jhydrol.2019.01.011
Received 29 September 2018; Received in revised form 7 December 2018; Accepted 2 January 2019
Available online 11 January 2019
0022-1694/

Watershed-level surface water supply consists of local water (i.e., surface and shallow subsurface runoff generated within each watershed that equals the difference between precipitation and ET at a multi-annual scale) and the amount of water accumulated from upstream river networks or transferred by artificial aqueducts. Compared to water resources generated from local precipitation, the non-local waters are not only restricted by the topography and infrastructure, but also susceptible to environmental changes and human activities in source areas (e.g., drought, water contamination, consumptive use). Although there have been a few studies assessing water stress in the U.S. under future climate, little attention has been paid to the role of water connectivity among regions. Some of the previous studies weighed water demand against supply at large basin scale, e.g., the U.S. was divided into 98 basins in Foti et al. (2012) and 99 basins in Blanc et al. (2014). Coarse-scale evaluation tends to underestimate stress by averaging the withdrawals and supply data (Oki et al., 2001; Vörösmarty et al., 2000), and the water movement in hydrologically connected areas is also masked. Given the lack of local control over upstream flow, some recent studies projected water availability and stress from a local perspective. For example, Devineni et al. (2015) used local precipitation at the county level to estimate renewable water supply and evaluated water stress as the ratio of water deficit (i.e., demand minus supply) to average rainfall; Roy et al. (2012) estimated renewable regional water supply with the available precipitation, defined as the difference between precipitation and potential evapotranspiration. These studies have shown merits in improving spatiotemporal resolutions and accounting for uncertainties with more sophisticated risk assessment approaches. However, the potential variations in water exchange among different areas were not considered, and consequently, the impact of climate change on water stress could be over or under-estimated.

This study aims to establish an integrative simulation and evaluation framework that incorporates the natural and anthropogenic water connections among the 2099 8-digit Hydrologic Unit Code (HUC-8) watersheds (http://water.usgs.gov/GIS/huc.html) across the conterminous United States (CONUS), and use it to investigate regional water availability and water stress in historical and future scenarios. Specifically, our goal is: (1) to investigate the role of water connections among watersheds (i.e., stream flows in river channels, artificial water transfers, water withdrawals and return flows) in distributing water supply, (2) to project the responses of water stress to climate change, socioeconomic status associated with climate change, and mitigation practices over the course of the 21st century, and (3) to examine the relative importance of driving factors from demand and supply aspects in impacting water stress at a high spatial resolution.

2. Methods

2.1. Hydrologic unit system and water connections

The hydrologic unit system developed by the United States Geological Survey (USGS) includes six levels of hydrologic units. Each unit is identified by a unique code consisting of two to twelve digits. The first level of classification divides the CONUS into 18 2-digit HUC areas, which are commonly referred to as Water Resource Regions (WRRs) (Fig. 1a). These regions can be further divided into 2099 8-digit HUC watersheds. The full lists and boundaries of hydrologic units at different levels can be found in the Watershed Boundary Dataset (https://datagateway.nrcs.usda.gov/).

The geospatial attributes of streams at different levels can be obtained from the National Hydrography Dataset (http://nhd.usgs.gov/data.html). We assumed that the outlet of each watershed (i.e., the inlet of the next downstream watershed) was the exiting reach with the greatest cumulative drainage area within the watershed, and thus identified a total of 18,777 upstream-downstream connections among HUC-8 watersheds (Caldwell et al., 2012; Emanuel et al., 2015). We categorized the 2099 HUC-8 watersheds into four types to specify the potential sources of water supply (Duan et al., 2018): (1) 'headwater' watershed, including 907 (43%) watersheds that are connected to downstream only; (2) 'midstream' watershed, including 779 (37%) watersheds that are connected to both upstream and downstream; (3) 'terminus' watershed, including 94 (5%) watersheds that are connected to upstream only; (4) 'isolated' watershed, including 319 (15%) watersheds that are not connected to either upstream or downstream. It can be assumed that only 'midstream' and 'terminus' watersheds would receive natural flows from upstream.

An addition of 228 artificial connections were identified based on historical inter-basin water transfers (IBTs) reported by Petsch (1985) and Mooty and Jeffcoat (1986). A total of 22 billion m^3 water per year has been transferred based on records from 1973 to 1982, which only accounts for ~1% of total water supply in the entire CONUS (Duan et al., 2018). However, these IBTs, ranging from 500 m^3 to 4 billion m^3 per year, have played an important role in securing regional water supply (e.g., San Joaquin and Colorado transfers for southern California; Delaware-Hudson transfer for New York City) and have widely impacted streamflow in areas downstream of the watersheds supplying/receiving IBTs (Fig. 1b).

2.2. Projection of water supply

Water supply was simulated dynamically at HUC-8 scale based on hydro-climatic modeling and the water connections among watersheds. First, hydrologic processes within each watershed was modeled under historical and future climate scenarios; second, water demand and consumptive use were projected at each county by water-use sectors and rescaled to HUC-8 level; and then, water withdrawals, return flows, and IBTs were implemented into the streamflow routing procedure to estimate regional water availability.

2.2.1. Watershed water balance

The HUC-8 level water balance was modeled with a previously validated monthly hydrologic model – the Water Supply Stress Index model (WaSSI). WaSSI was developed to capture land-cover specific large-scale water balance in the CONUS, i.e., the processes of snowpack melt/accumulation, soil moisture accounting, evapotranspiration, and runoff generation (Caldwell et al., 2012; Sun et al., 2011; Sun et al., 2008). It has been widely used in the U.S. (Duan et al., 2017a), Africa (McNulty et al., 2016), and China (Liu et al., 2013). The extensive validation with USGS measured streamflow (Caldwell et al., 2015; Duan et al., 2017b; Sun et al., 2015b) and remote sensing products of ET and ecosystem productivity (Sun et al., 2011; Sun et al., 2015b) suggest that WaSSI can achieve an acceptable modeling accuracy with respect of both water and carbon fluxes at broad spatial scales.

Two climate datasets were used to drive the hydrologic model: (1) monthly precipitation and temperature for the historical period of 1961–2010 from the Parameter-elevation Relationships on Independent Slopes Model (PRISM) dataset (http://prism.oregonstate.edu/) (Daly et al., 2008), and (2) monthly precipitation, maximum and minimum temperature, solar radiation, wind speed, and specific humidity from the Multivariate Adaptive Constructed Analogs (MACA) datasets (the MACAv2-LIVNEH dataset, available at http://maca.northwestknowledge.net/) (Abatzoglou and Brown, 2012; Livneh et al., 2013). The MACA data includes downscaled and bias-corrected climate from 20 Global Climate Models (GCMs) of the fifth phase of the Coupled Model Inter-comparison Project (CMIP5). It spans from 1950 to 2099 to include the experiments of 'historical', Representative Concentration Pathways (RCP) 4.5, and RCP8.5, which correspond to the climate forcings (i.e., greenhouse gases emissions, aerosols, land-use feedbacks, etc.) observed in the history and projected in a future with the radiative forcing reaching 4.5 and 8.5 W m^{-2} in 2100 (equivalent to 650 ppm and 1370 ppm CO_2), respectively (IPCC, 2014; Moss et al., 2010). More details of the modeling approaches and results of water balance components derived from these climate datasets can be found

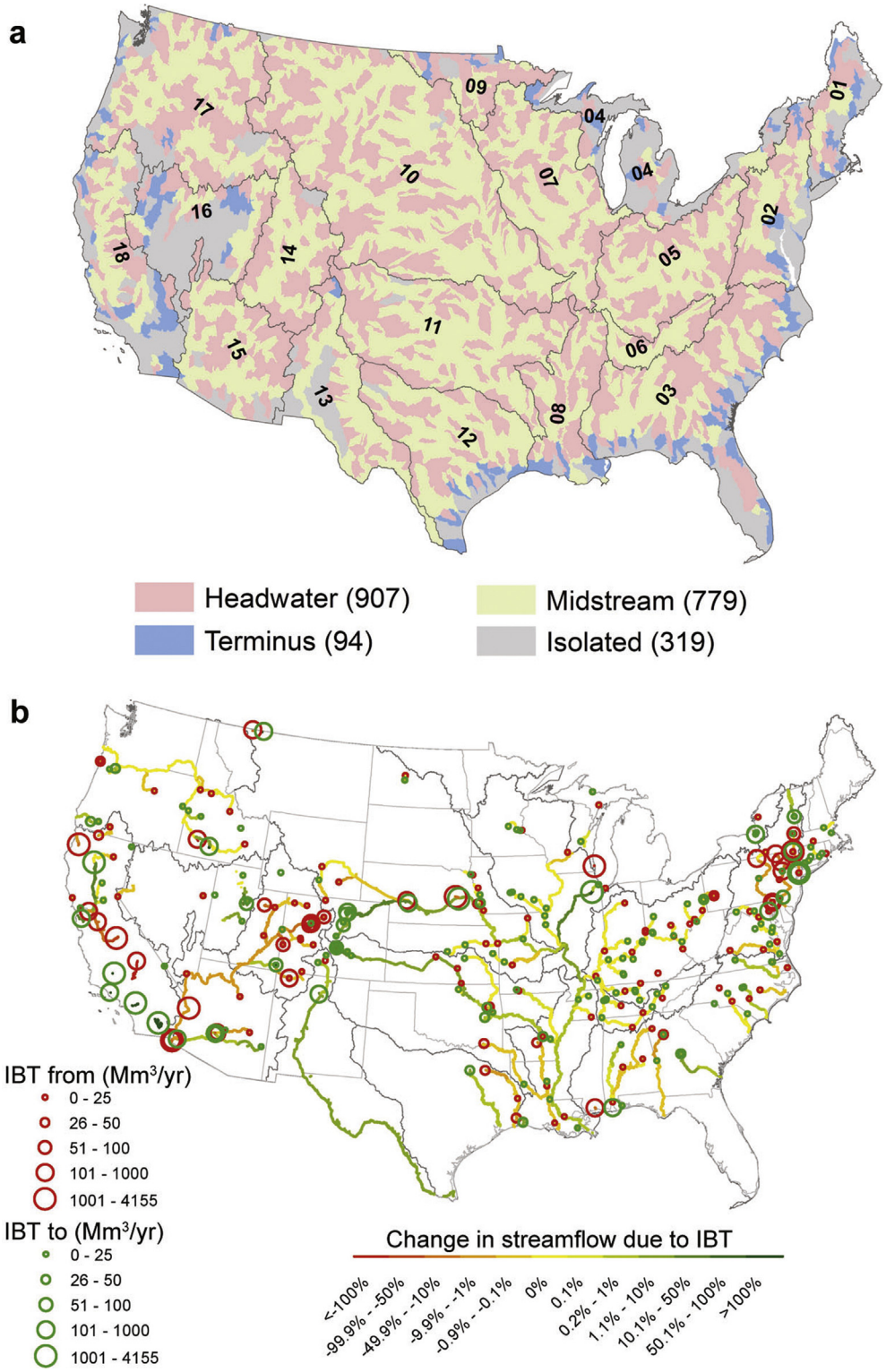

Fig. 1. Water connectivity among 2099 8-digit Hydrologic Unit Code (HUC-8) watersheds in the conterminous United States (CONUS). a, Distribution of "headwater," "midstream," "terminus", and "isolated" watersheds in the 18 water resource regions (numbers of these watersheds are marked with brackets in the legend); b, Location of inter-basin water transfers (IBTs) and their impacts on streamflow (adapted from Emanuel et al., 2015). The magnitudes of IBTs are the averages from 1973 to 1982, and the changes in mean annual streamflow is relative to the average from 2000 to 2010.

in a previous study (Duan et al., 2017b).

2.2.2. Streamflow routing and regional water supply

The total available surface water supply (total flow, *TF*) for a watershed was simulated as

$$TF = LF + \sum_{i=1}^{N} UF_i - \sum_{i=1}^{N} UWC_i \pm IBT \quad (1)$$

where local flow (*LF*) equals the runoff generated within the target watershed, which can be interpreted as precipitation (*P*) minus ET and changes in soil moisture (*SM*) and hydrologically connected snowpack

(*SP*):

$$LF = P - ET + dSM/dt + dSP/dt \quad (2)$$

$\sum_{i=1}^{N} UF_i$ is the sum of runoff accumulated from all the connected upstream watersheds, while $\sum_{i=1}^{N} UWC_i$ represents the sum of water consumption in these watersheds that equals water withdrawals minus return flows. Water withdrawals and consumptive uses were assumed to occur uniformly in each watershed. The residuals of upstream flow after consumptive uses were assumed to be discharged simultaneously to surface water at the inlet of the next downstream watershed. In the cases that the accumulated streamflow cannot meet the demand, the actual water withdrawal was set to equal the maximum water availability, and consumptive use and the return flow discharged to downstream were downsized with the same ratio. The watersheds supplying IBTs were assumed to meet the need of water transfer before local withdrawal. Magnitudes of the IBTs were also reduced to the maximum water availability in the cases of water deficit, and the same ratio was implemented for all the transfers if a watershed was supplying IBTs to multiple watersheds. The regulations of dams and reservoirs were not included in this study because most of these facilities are operated on seasonal or monthly basis, while this study aims to provide a long-term projection at annual and decadal scales.

2.3. Projection of water withdrawal and consumption

Projection of future water demand was based on the extrapolation of past trends and the estimates of demographic, economic, and climatic forces on water uses. National water-use data from 1950 to 2010 by 5-year interval (county-level data is available from 1985 to 2010) were obtained from the USGS water census reports (available at http://water.usgs.gov/watuse/data/). We here focus on the potential changes in the thermoelectric, irrigation, and domestic (including self-supplied and public delivered) sectors. In 2010, these three sectors accounted for 84% of the total surface freshwater withdrawal in the CONUS (i.e., 50% thermoelectric, 28% irrigation, and 6% domestic) (Maupin et al., 2014). County-level withdrawal and consumption in the other sectors, including livestock, aquaculture, industrial, and mining, were included but were assumed to remain at the same levels as 2010 through the 21st century. The ratios of surface freshwater withdrawal to total water withdrawal (i.e., surface freshwater plus groundwater and saline water) were assumed to remain constant.

2.3.1. Domestic use

Per capita domestic water use in the U.S. has been relatively stable since 1990 (Maupin et al., 2014), but the total domestic water demand is likely to further increase if population grows. In this study, per capita domestic water withdrawal and consumption in each county were assumed to remain at the same levels as in 2010. Domestic uses in the future were estimated by multiplying the per capita use in 2010 by the population projected for the period of 2010–2100. The proportions of public and self-supplied domestic uses were also assumed to be constant over time.

Population projections in the 3109 counties over the CONUS were obtained from the Integrated Climate and Land-Use Scenarios (ICLUS) v1.3 datasets that compiled by the U.S. Environmental Protection Agency (EPA) (https://www.epa.gov/iclus/iclus-downloads). This projection links demographic models with the climate and land-use changes from the Intergovernmental Panel on Climate Change's (IPCC) Special Report on Emissions Scenarios (SRES) of social, economic, and demographic storylines. The total population in the CONUS is projected to increase from 310 million in 2010 to 402–688 million in 2100 among the SRES scenarios (A1, rapid economic growth; A2, regionally oriented economic development; B1, global environmental sustainability; and B2, local environmental sustainability). Outputs under B1 and A2 scenarios, which are comparable to the emission scenarios of RCP4.5 and RCP8.5 used in the fifth IPCC report, were used to represent the low and high population projections, respectively.

2.3.2. Thermoelectric use

Thermoelectric water demand was estimated as total thermoelectric power generation multiplying per kWh water use. The electric power projections in 2010–2040 were obtained from the Annual Energy Outlook provided by the Energy Information Administration (EIA) of U.S. Department of Energy (DOE) (2016). The outputs include electricity generated in the fossil fuels and nuclear power plants in the 22 Electricity Market Module (EMM) regions in the CONUS under two reference scenarios with and without complying with the Clean Power Plan (CPP). The CPP is a U.S. EPA program issued under the Clean Air Act (42 U.S.C. §7401), which requires a reduction in carbon emission from current fossil fuel plants (by 32% until 2030) and an extension of tax credits for renewable energy (currently under review, https://www.epa.gov/economic-and-cost-analysis-air-pollution-regulations/regulatory-impact-analysis-review-clean-power). The power generation data for each EMM region was linearly extrapolated forward from 2041 to 2099 using the average rates of change in 2010–2040. The regional data was then disaggregated to HUC-8 watersheds based on two assumptions (Roy et al., 2012): (1) the increase/decrease in power generation only occurs in watersheds with existing thermoelectric plants, and (2) the same changing rate against the 2010 level is applied to all the watersheds within each EMM region. We did not consider the additional impact of climate warming on electricity demand for air conditioning because: (1) the electricity demand did not show a clear correlation with climatic drivers at the national scale according to the EIA datasets, and (2) future behavioral responses to climate change may be largely affected by the evolving air conditioning technology and market saturation (Sailor, 2001; Sailor and Pavlova, 2003).

Water use per kWh has been decreasing in recent decades due to the improvement of technology, especially the movement from once-through (or 'open-loop') to recirculation (or 'closed-loop') cooling system. Once-through cooling accounted for 94% of total water withdrawals and 47% of power generation in 2010, while plants with recirculation systems generated the other 53% power with only 6% withdrawal (Maupin et al., 2014). This decreasing trend in per kWh withdrawal is likely to continue in the foreseeable future as industry regulations will continue to encourage cooling systems with lower withdrawal requirements. However, it should be noted that the water consumption of a recirculation system is generally larger than that of a once-through system. Higher consumption is expected under future scenarios with a larger share of power plants converting to a recirculation system, even though water withdrawal is projected to decrease (Feeley et al., 2008). The projections conducted by the National Energy Technology Laboratory (NETL) (2011) suggested that total water consumption would increase between 2010 and 2035 under all of the five scenarios accounting for different additions and retirements of thermoelectric generating capacity and cooling systems (including once-through, recirculation, and dry cooling systems). We used the average changing rates of water withdrawal per kWh and water consumption per unit withdrawal under these five scenarios to represent the future changes from 2010 to 2035, and extrapolated these trends forward to 2099 by EMM region. Similar to the disaggregation of power generation, the same changing rates against the baseline level in 2010 was applied to all the watersheds with existing thermoelectric plants within each EMM region.

2.3.3. Irrigation use

Irrigation water demand was calculated as irrigated area multiplying irrigation use per unit area (i.e., irrigation efficiency). Considering the changing needs for agricultural crops and the increasing evaporative demand caused by warming, future irrigation water demand (*WI*) is estimated by the changes against the 2010 level, as

$$WI = \alpha \times WI_{2010} \times (I_{net}/I_{net2010}) \quad (3)$$

where I_{net} is net irrigation water demand per unit area and $I_{net}/I_{net2010}$ indicates its change caused by climate change. The correction coefficient α is used to represent the potential changes in irrigated area (A) and irrigation efficiency (η) without the impact of climate change, as

$$\alpha = (A \times \eta)/(A_{2010} \times \eta_{2010}) \quad (4)$$

Irrigated area and irrigation efficiency are affected by a complex mixture of socioeconomic factors such as agricultural policies, irrigation technology, and crop market. Due to the lack of local-level information on these factors, we used the WRR-level projections suggested by Brown et al. (2013), and assumed that changes in irrigated area and irrigation water demand would only occur in watersheds with existing irrigated agriculture. Based on the historical records of irrigated area, irrigation water withdrawal, and distribution of irrigation systems (e.g., surface flood, sprinkler, and micro-irrigation) from the USGS, Brown et al. (2013) extrapolated the past trends and developed two sets of estimates for the east (WRR#1–#9) and west (WRR#10–#18) of the CONUS. The majority of the total irrigation withdrawals occurred in 17 western states (e.g., Nebraska, California, Idaho) where annual precipitation was less than 20 in. (Maupin et al., 2014). Irrigated area in the west is projected to continue the decreasing trend begun in the 1980s. The improvements in irrigation efficiency have caused a notable decline in the irrigation withdrawals both in the west and for the entire CONUS. Sprinkler and drip irrigation have already been widely used in the west, but finer micro-irrigation techniques or new methods may be developed as a response to the aggravated water deficit in a warmer future. In the east, irrigated area is projected to continue to increase but at a decreasing rate, and sprinkler and drip systems are expected to gradually replace surface flooding in humid states. The combination of the changes in irrigated area and irrigation efficiency will cause the α coefficient to decrease in the west but increase in the east.

I_{net} is estimated by the difference between evaporative demand and supply (Döll, 2002; Döll and Siebert, 2002), as

$$\begin{aligned} I_{net} &= k_c \times PET - Pe \quad \text{if } PET > Pe \\ I_{net} &= 0 \quad \text{if } PET \leqslant Pe \end{aligned} \quad (5)$$

where PET is potential evapotranspiration calculated with the Penman-Monteith method (Allen et al., 1998); kc is a crop coefficient, which is set to 1 as we are not differentiating crop types (Brown et al., 2013); Pe is effective precipitation representing the fraction of precipitation and snowmelt that is available to crop and does not run off. Pe is estimated with a simplified empirical relationship with precipitation (P) – the USDA Soil Conservation Method (Smith, 1992), as

$$\begin{aligned} Pe &= P(125 - 0.2P)/125 \quad \text{if } P < 250\,\text{mm/month} \\ Pe &= 125 + 0.1P \quad \text{if } P \geqslant 250\,\text{mm/month} \end{aligned} \quad (6)$$

We assumed a constant 6-month growing season from April to September. The mean monthly P and PET during the growing season were used to estimate Pe and I_{net}. The future changes in plant species and cropping structure, and the potential lengthening/shortening of the growing season caused by climate change were not considered.

The impact of changing irrigation methods on irrigation water consumption is not entirely clear and difficult to quantify without on-site observations. However, there has been rising concern that the adoption of more efficient irrigation technologies (e.g., from flood to drip), which requires less water to be withdrawn, could also cause larger consumptive rates and reduce valuable return flows (Ward and Pulido-Velazquez, 2008). For example, Hu et al. (2017) found a strong inverse linear correlation ($r = -0.99$, $p < 0.01$) between irrigation return flow coefficient (return flow/water applied) and irrigation efficiency in an experimental cotton plantation. Therefore, we assumed that water consumption per unit area would remain at the same levels as in 2010 in irrigated areas, i.e., water consumption per unit withdrawal would increase accordingly as the updates of irrigation system decrease withdrawal per unit area.

2.4. Water stress evaluation

2.4.1. Stress indices and classification

Two indices of water stress were used to address the sufficiency of local and non-local water resources in meeting water demand (Duan et al., 2018):

- Local Water Stress (*LWS*), defined as the ratio of *WD* to *LF*;
- Global Water Stress (*GWS*), defined as the ratio of *WD* to *TF*.

Water stress is usually considered high when the ratio of withdrawal to supply exceeds 0.4 due to the concern that water demands for in-stream uses, such as navigation, hydropower generation, and ecological and environmental demands, should also be met (Oki et al., 2001; Richey et al., 2015; Vörösmarty et al., 2000). We here further define three levels of stress using 0.4 as the threshold value, including:

- 'Unstressed', represents a condition without water stress that local water resource alone can suffice the demand, identified if $LWS < 0.4$;
- 'Upstream-stressed', represents a condition that sufficient water supply is dependent on the availability of upstream water (or water transferred though artificial aqueducts), identified if $LWS > 0.4$ & $GWS < 0.4$;
- 'Overstressed', represents a condition with high water stress even when water supply is complemented by upstream water (or transferred water), identified if $GWS > 0.4$.

2.4.2. Scenarios of water stress

We reconciled the datasets of population, electricity generation, climate, and water uses from different sources to provide a projection of future water demand, supply, and stress at the HUC-8 level. Although the underlying assumptions of these datasets are not entirely consistent, they are all closely related to climate change and the associated mitigation measures. We focused on two future scenarios of water stress in our analysis (Table 1): (1) intermediate stress (IS), driven by population under B1, climate under RCP4.5, and power generation with the CPP, and (2) high stress (HS), driven by population under A2, climate under RCP8.5, and power generation without the CPP. The IS and HS scenarios represent a future with and without climate change mitigation strategies, respectively. The average IBT magnitudes derived from the data in 1973–1982 were used through all of the time periods under both future scenarios. The historical scenario (1981–2010) based on the

Table 1
Summary of historical (1981–2010) and future (2011–2099) scenarios of water supply stress.

Scenario	Water supply	Water demand		
		Domestic	Thermoelectric	Irrigation
Historical	PRISM climate	USGS county-level census		
Intermediate Stress (IS)	Climate under RCP4.5	Population under SRES B1	Electricity generation with Clean Power Plan	Climate, PET, and ET under RCP4.5
High Stress (HS)	Climate under RCP8.5	Population under SRES A2	Electricity generation without Clean Power Plan	Climate, PET and ET under RCP8.5

PRISM climate data and USGS water use census reports was used as a benchmark for identifying changes in the future.

2.4.3. Attribution of potential changes in water stress

The potential changes in *GWS* are attributed to the impacts of water demand (*WD*) and total water supply (*TF*) as

$$\Delta GWS = \frac{1}{TF}\Delta WD - \frac{WD}{TF^2}\Delta TF + \frac{WD}{TF^3}(\Delta TF)^2 \quad (7)$$

where ΔGWS is the change in the ratio of WD/TF; $\frac{1}{TF}\Delta WD$ is the contribution of *WD* change; the sum of the second and third terms on the right side of the equation is the contribution of *TF* change (Feng and Fu, 2013). The demand contribution is further attributed to water-use sectors of domestic, thermoelectric, and irrigation, while the supply contribution is attributed to changes in local flow (*LF*), upstream flow (*UF*), and upstream water consumption (*UWC*) by their weights in *TF* change.

3. Results

3.1. Projected changes in water demand, supply, and stress

3.1.1. National scale

The CONUS population is projected to increase from 310 to 392 and 669 million under the SRES B1 and A2 scenarios by 2099, respectively. Consequently, domestic water demand (Fig. 2a) is projected to increase from 2×10^{10} to 2.7×10^{10} (IS) and 4.9×10^{10} m^3 (HS) from 2011 to 2099, with a quarter of the withdrawn water being consumed (Fig. 2b). Thermoelectric power generation is projected to drop between 2010 and early 2020s due to the growing role of renewable energy (e.g., solar, wind, geothermal). The decreasing trend is expected to continue under the CPP scenario and result in a reduction in thermoelectric withdrawal from 1.4×10^{11} (2011) to 1.1×10^{11} m^3 (2099) (Fig. 2c). However, under the scenario without the CPP, the total thermoelectric water use is likely to increase again after 2020s because of the increasing electricity demand, and exceed the 2010 level in the 2070s in spite of the decreasing per kWh withdrawal. Water consumption in the thermoelectric sector (Fig. 2d) will increase from 9×10^9 in 2011 to 1.1×10^{10} m^3 in 2099 with the CPP as a result of the rising consumption rate, whereas a more significant increase by 5×10^9 m^3 (from 9×10^9 to 1.4×10^{10} m^3) is projected under the scenario without the CPP. Projections of irrigation use (Fig. 2e) show highly diverse variations among the climate models. Multi-model means under RCP4.5 suggest relatively smaller changes in irrigation withdrawal and consumption, fluctuating around 9×10^{10} m^3 and 5×10^{10} m^3 respectively. Meanwhile, clear increasing trends are projected under RCP8.5, with withdrawal and consumption reaching 1.4×10^{11} m^3 and 7×10^{10} m^3 by the end of this century.

Combining the projected changes in domestic, thermoelectric, and irrigation withdrawals, total water demand in the CONUS (Fig. 3a) is

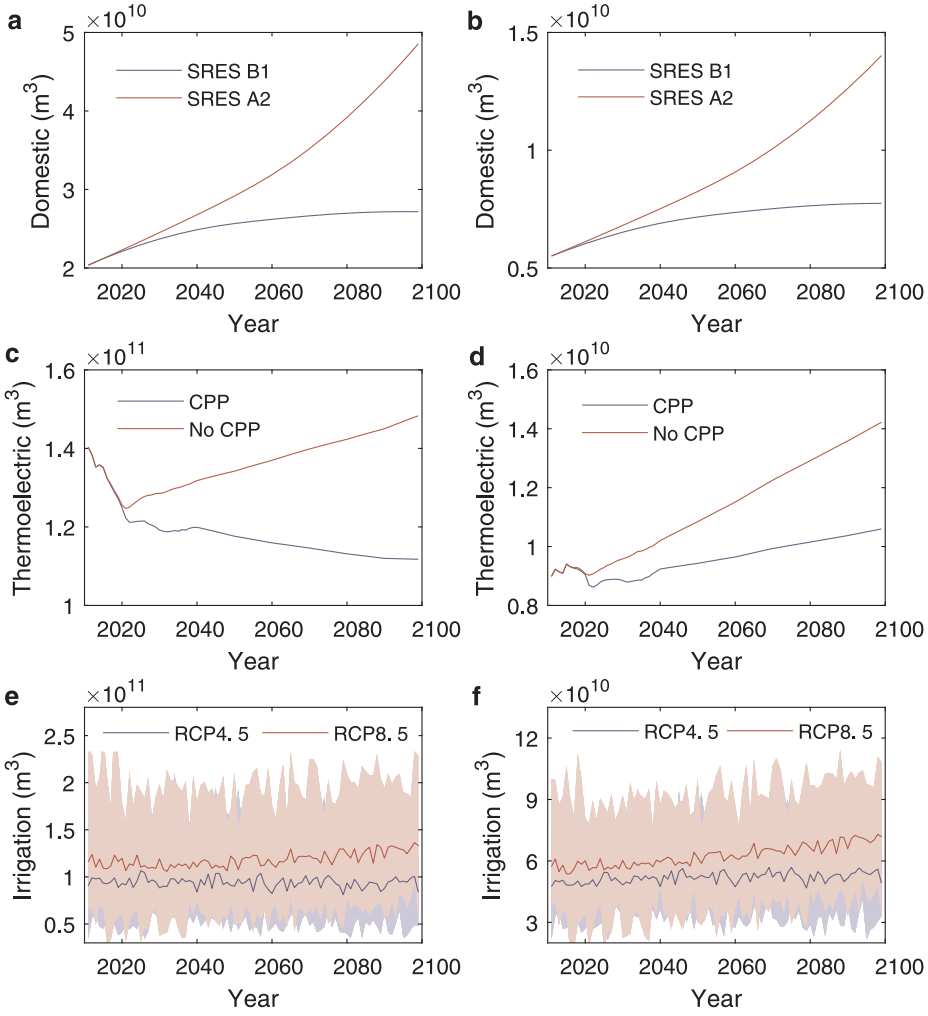

Fig. 2. Projected annual water withdrawal (Fig. a, c, e) and water consumption (Fig. b, d, f) in the sectors of domestic, thermoelectric power generation, and irrigation over the CONUS in the period of 2011–2099. Fig. e–f displays the uncertainty ranges (shadings) and ensemble means (lines) derived from multiple climate models.

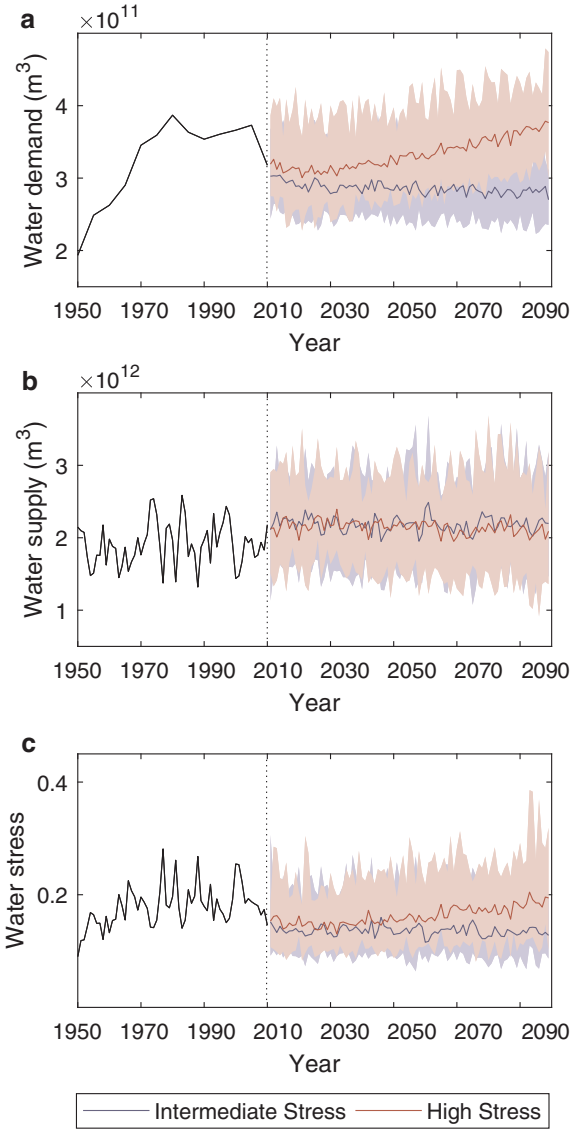

Fig. 3. Overall annual water demand, supply, and stress in the CONUS from 1950 to 2099 under the scenarios of Intermediate Stress (IS) and High Stress (HS).

projected to increase from 3.2×10^{11} m^3 in 2010 to 3.8×10^{11} m^3 in 2099 under the HS scenario. Conversely, a notable reduction by 0.5×10^{11} m^3 in total demand is expected under the IS scenario due to the decrease in thermoelectric withdrawal. On the other hand, total water supply (the sum of annual *LF* over the CONUS) (Fig. 3b) derived from the ensemble mean of multiple climate models shows a slight decrease under both IS (-3×10^8 m^3 yr^{-1}, $R^2 = 0.01$) and HS (-1×10^9 m^3 yr^{-1}, $R^2 = 0.11$). Judging by the multi-decadal average in 2070–2099, significantly larger demand ($+7.6 \times 10^{10}$ m^3 yr^{-1}) and smaller supply (-8.0×10^{10} m^3 yr^{-1}) are projected under the HS than that under the IS. It should be kept in mind that these multi-model means can only represent hydrologic responses to the averaged climate forcings in the future. The natural climate fluctuations and the uncertainties in climate models lead to large variability in annual water supply and demand (e.g., supply and demand respectively vary between 1.4–3.2 $\times 10^{12}$ m^3 and 2.4–4.7 $\times 10^{11}$ m^3 in 2099).

Overall water stress (ratio of total demand to total supply) (Fig. 3c) is projected to change divergently under the two future scenarios. Results of multi-model means suggest that water stress is likely to fall between 0.13 and 0.15 in most of the years under the IS scenario (-6×10^{-5} yr^{-1}, $R^2 = 0.03$). However, a pronounced rise from 0.15 in 2011 to 0.19 in 2099 is expected under the HS scenario ($+5 \times 10^{-4}$ yr^{-1}, $R^2 = 0.67$), driven by the increasing demand and decreasing supply. The highest stress over 0.39 was found in the projections based on the BCC-CSM1.1-m climate model. These differences between the results under the IS and HS scenarios suggest that the implementation of emission mitigation measures, including the CPP program and other socio-economic developments associated with SRES and RCP scenarios, would largely alleviate water stress from both demand and supply aspects.

3.1.2. Watershed scale

Fig. 4 shows the spatial variation of multi-decadal changes in water demand (*WD*) and supply (*TF*) from 1981 to 2010 to 2070–2099. Multi-model mean and consensus among the climate models were used to evaluate the future changes and associated uncertainties. An increase or decrease is considered significant (i.e., high consensus) when results derived from over 80% of the climate models agree on the changing sign. Under the IS, a significant decrease in *WD* will occur in over half of all the watersheds, while an increase is projected to scatter in another one fifth of the watersheds. Areas with an increasing *WD* are expected to expand significantly to cover one third of the CONUS under the HS. *TF* change shows extensive decreases in the western and central regions (WRR#10–#18), and high consensus is found in 864 and 850 out of the 2099 watersheds under the IS and HS scenarios. Significant increases in *TF* are mainly found in the east (WRR#1–#6) and Pacific coast (WRR#17 Pacific Northwest), and cover 17%–23% of the CONUS.

High consensus on *GWS* change (Fig. 5a–c) is projected in 1520 (587 increases and 933 decreases) and 1472 (833 increases and 639 decreases) watersheds under the IS and HS scenarios, respectively. Under the IS, decreasing *GWS* covers a majority of the eastern CONUS while a significant increase can be mainly found in the west. The coverage of increasingly stressed area is expected to be clearly larger under the HS, and fewer decreases in stress are also projected in the east. In particular, a noticeable shift from increase to decrease in *TF*, and from decrease to increase in *GWS*, can be found across the south (WRR#12 Texas-Gulf) and southeast (WRR#3 South Atlantic Gulf, WRR#8 Lower Mississippi) when comparing HS to IS.

We also compared the results of water stress interpreted by *GWS* and *LWS* to quantify the benefits of water produced upstream and water artificially transferred across the country (Fig. 5d–f). In the historical period, 12% more land area of the CONUS would face high stress if only local water was available. A total of 743 and 951 increasingly stressed watersheds are identified by *LWS* under the IS and HS scenarios, respectively, which are 27% and 14% more than that by *GWS*. Such results demonstrate the role of upstream water and transferred water in reducing the sensitivity of stress to future changes, particularly the potential stress escalations in the western regions.

3.2. Contributions of the driving factors

We further analyzed the contributions of demand (i.e., domestic, thermoelectric, irrigation) and supply (i.e., *LF*, *UF*, *UWC*) factors in altering *GWS* from 1981 to 2010 to 2070–2099 for each watershed. Changes in domestic demand (Fig. 6a–b) caused by population growth and migration are identified as the largest contributor in 12% (under IS) and 15% (under HS) of the CONUS area, mostly distributed in southern California (WRR#18) and the southwest (WRR#12 Texas-Gulf, WRR#13 Rio Grande, WRR#15 Lower Colorado). The changing thermoelectric demand (Fig. 6c–d) is projected to increase stress in the east (WRR#1–6) and the south (WRR#8 Lower Mississippi, WRR#11 Arkansas-White-Red, WRR#12 Texas-Gulf), while alleviating stress across the rest of the country. Domestic and thermoelectric demands tend to dominate stress changes in densely populated areas, such as the metropolitan areas in Texas (WRR#12) and Atlantic coastal regions (WRR#1–#3). These two driving factors are expected to be the largest

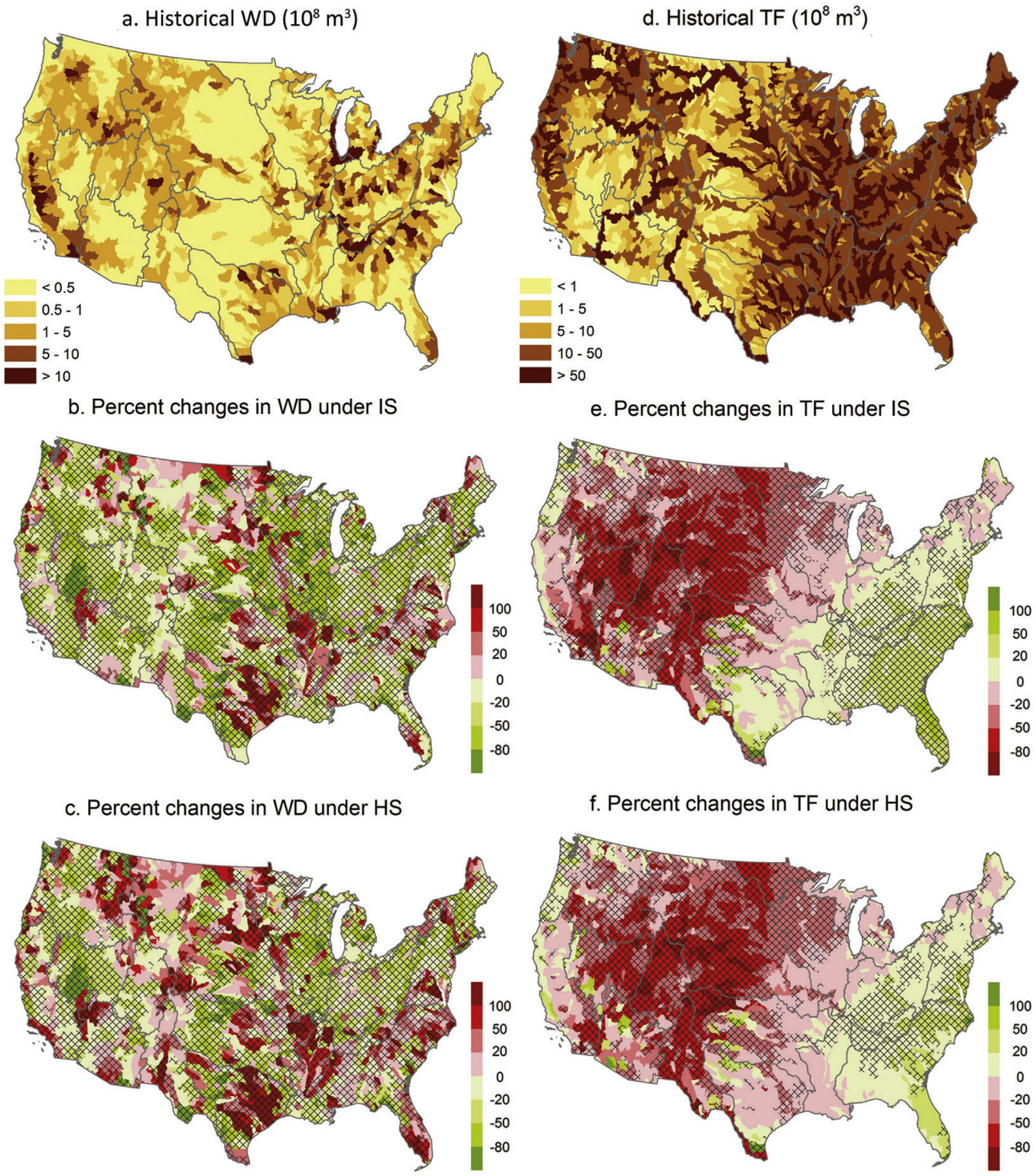

Fig. 4. Historical (1981–2010) and projected changes (2070–2099) in mean annual water demand (*WD*) (a–c) and total flow (*TF*) (d–f) across the HUC-8 watersheds under the scenarios of Intermediate Stress (IS) and High Stress (HS). The displayed changes are based on the ensemble means derived from the climate models. The watersheds are crosshatched where more than 80% of the models agree on the increasing/decreasing signal.

in 32%–34% of the CONUS that accounts for up to 60%–64% of the population under the future scenarios. Future changes in irrigation water use (Fig. 6e–f) are projected to aggravate stress in the east but alleviate stress in a large part of the west, as intensified water shortage may lead to decrease in irrigated area and more investment in irrigation techniques in the dry west. However, there is still notable increase in irrigation demand across most of the country under the HS scenario.

LF change induced by local climate change (Fig. 7a–b) is expected to be the major cause of water stress escalation in the west (WRR#10–18) and stress alleviation in the Atlantic coast (WRR#2–3), accounting for 24%–25% of the CONUS (10%–17% of the population). The effects of *LF* are enhanced by the consequent changes in *UF* (Fig. 7c–d) in watersheds involved with the river networks, generally driving water stress to increase and decrease in the west and east of Mississippi, respectively. *UF* change, driven by the combined effects of climate change in upstream areas, is recognized as the most influential factor in

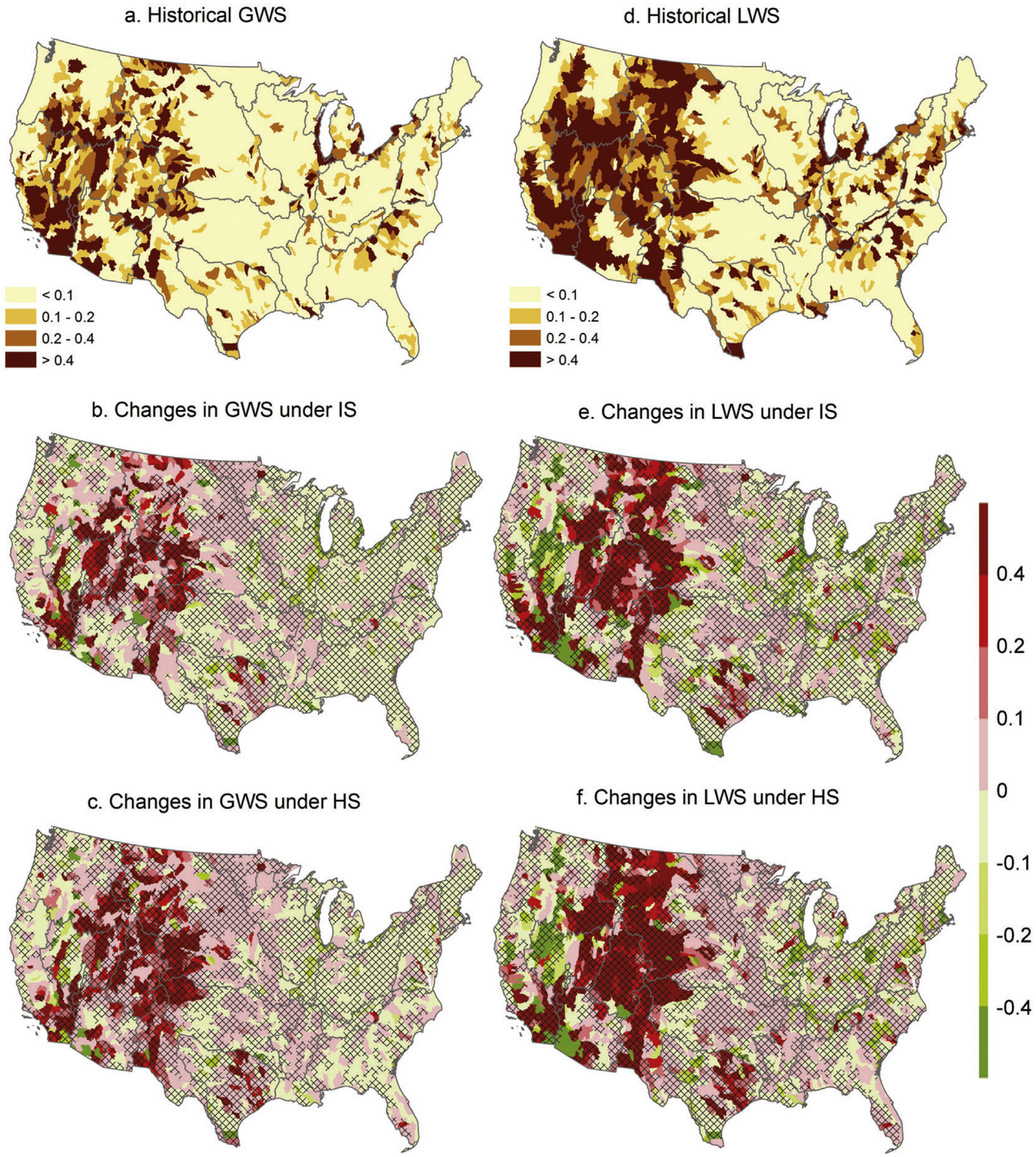

Fig. 5. Historical (1981–2010) and projected changes (2070–2099) in local water stress (*LWS*) (a–c) and global water stress (*GWS*) (d–f) across the HUC-8 watersheds under the scenarios of Intermediate Stress (IS) and High Stress (HS). The displayed changes are based on the ensemble means derived from the climate models. The watersheds are crosshatched where more than 80% of the models agree on the increasing/decreasing signal.

15%–16% of the area (9% of the population) that mostly distributed across large river basins in the west, such as the Missouri, Arkansas, Rio Grande, Gila, and Colorado Rivers. Contrary to the impact of *UF* change, *UWC* drives water stress to increase in the east as a result of the increasing water withdrawals, but will counterbalance the stress escalation widely across the river basins in the west of Mississippi (including Missouri, Mississippi, Arkansas, Canadian, Red, Brazos, Pecos, Rio Grande, and Gila river basins) as thermoelectric and irrigation water uses are projected to decrease. In 24–29 of these watersheds (1%–2% in area), which is mostly scattered across the Arkansas, Canadian, and Brazos river basins (WRR#10–12), *UWC* is projected to be the most influential factor.

We summarized the relative importance of the driving factors in water stress change across the watersheds by the four categories of hydrologic connectivity (i.e., 'headwater', 'midstream', 'terminus', and 'isolated') based on the multi-model mean results (Fig. 8). On average, water demand contribution ranges from 55% in 'midstream' watersheds to 70% in 'isolated' watersheds, with irrigation being the largest

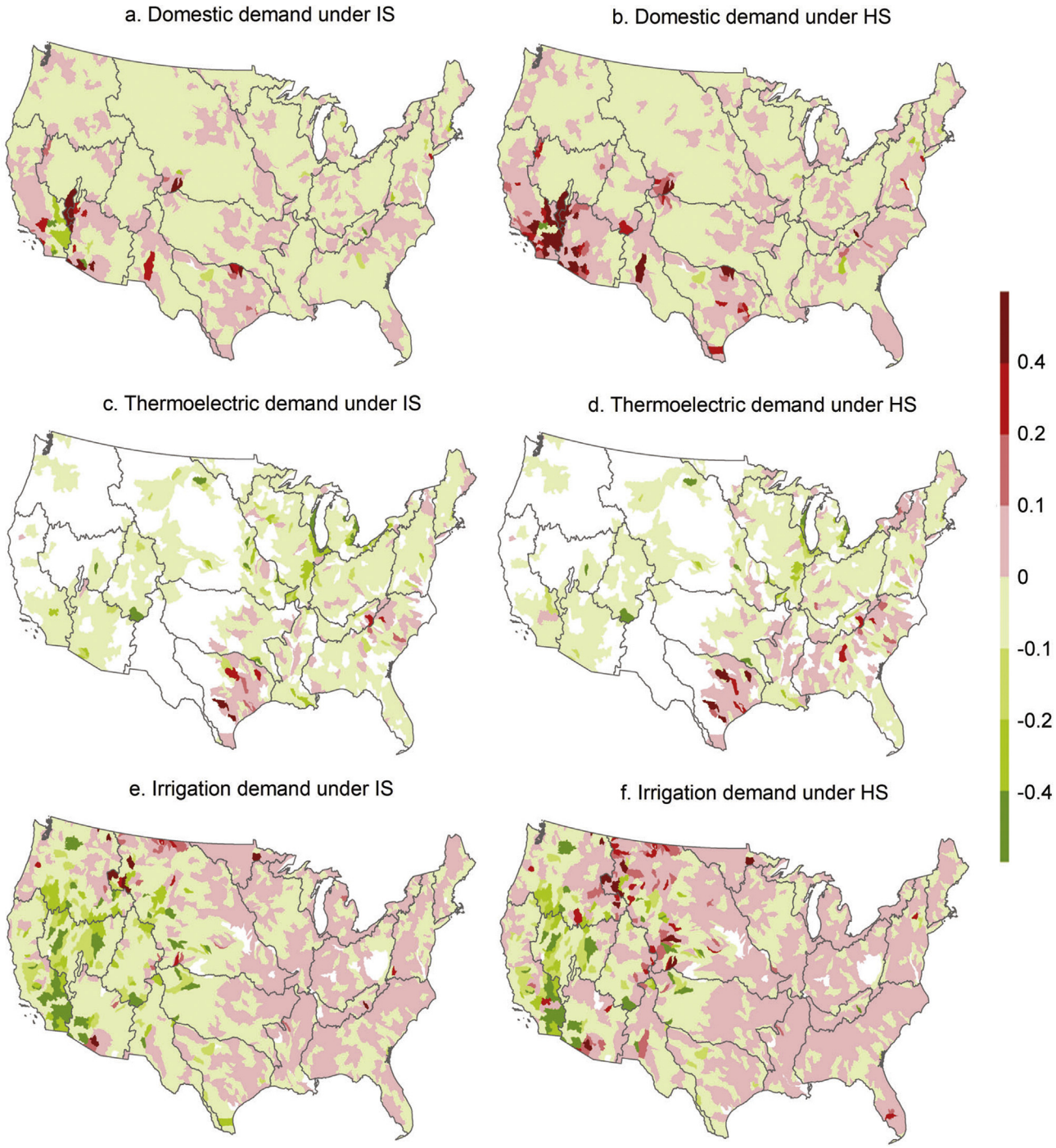

Fig. 6. Contributions of water demand in the sectors of domestic (a–b), thermoelectric power generation (c–d), and irrigation (e–f) to projected changes in water stress from 1981 to 2010 to 2070–2099 under the scenarios of Intermediate Stress (IS) and High Stress (HS) based on multi-model means.

contributing sector across all the categories (23%–32%). In terms of water supply, *LF* accounts for 30%–39% of stress change in 'headwater' and 'isolated' watersheds. Meanwhile, *UF* change is the most influential factor (21%–28%) for water supply in 'midstream' and 'terminus' watersheds, followed by *LF* (7%–10%) and *UWC* (4%–7%). Such results demonstrate the critical role of upstream water in securing water supply in 'midstream' or 'terminus' watersheds along large rivers, where changes in upstream climate and water consumption could exert a much larger impact on water stress than changes in local climate. A similar pattern of the six factors' relative importance is projected for the two future scenarios even though much higher stress is expected in the HS scenario.

3.3. Changes in stress level and coverages

Areas that relied on non-local water for adequate freshwater supply, defined as 'upstream-stressed' in this study, covered 10%–14% of the CONUS through the baseline period (1981–2010). Meanwhile, the areal extant of 'overstressed' areas, where high water stress was observed even when water supply is complemented by upstream flows or IBTs, varied widely between 9% and 20% from wet years to dry years. The ranges derived from the multiple climate models also suggest that much larger uncertainty is involved in the projection of 'overstressed' coverage (5%–39%) than that of 'upstream-stressed' (6%–15%) (Fig. 9). Judging by the ensemble means of multiple GCMs, there will be little

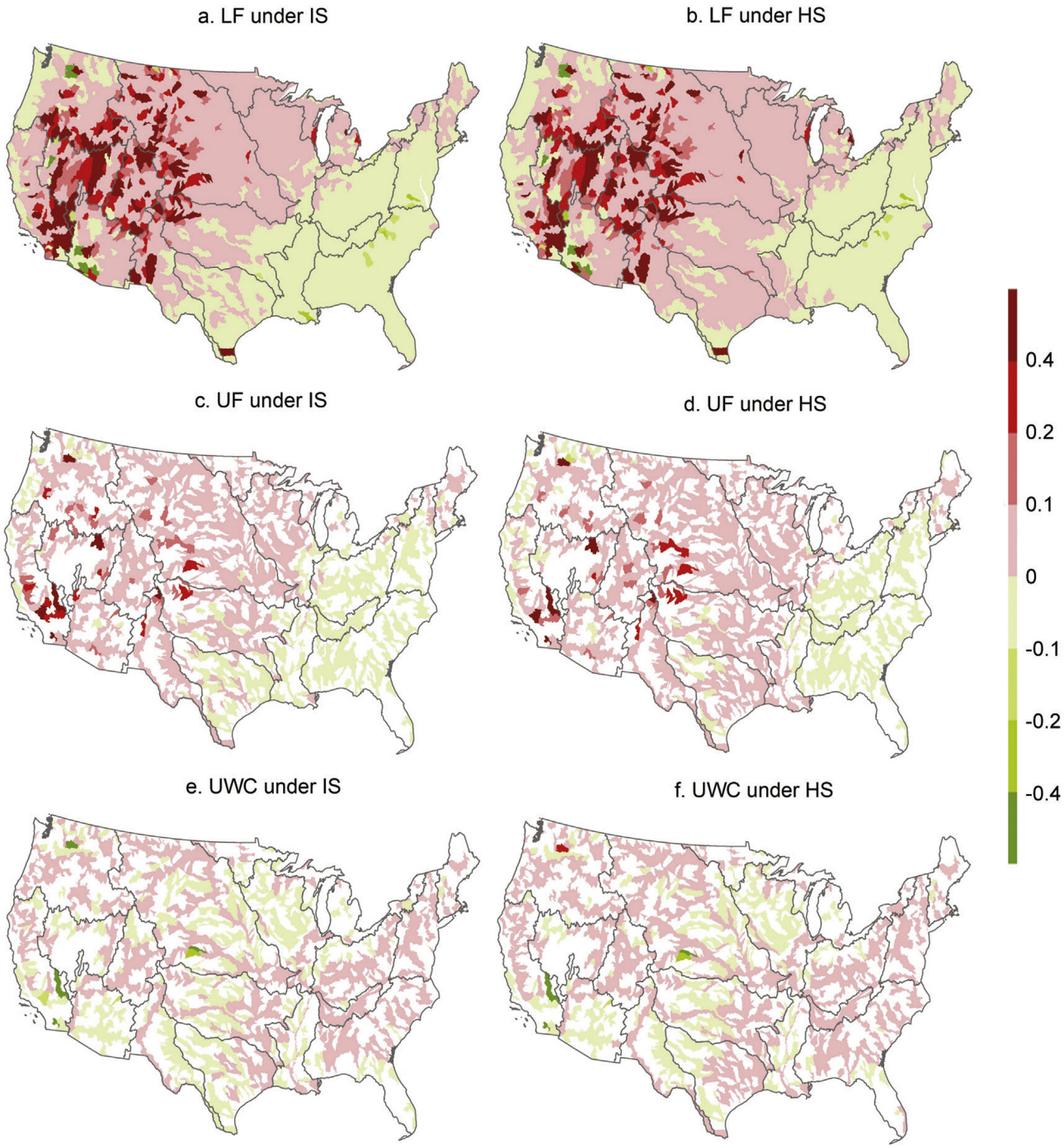

Fig. 7. Contributions of local flow (*LF*) (a–b), upstream flow (*UF*) (c–d), and upstream water consumption (*UWC*) (e–f) to projected changes in water stress from 1981 to 2010 to 2070–2099 under the scenarios of Intermediate Stress (IS) and High Stress (HS) based on multi-model means.

change in the overall stress coverage under IS, yet an evident expansion through this century under HS. On multi-decadal basis, 12% and 14% of the CONUS area (15% and 19% of the population) were identified as 'upstream-stressed' and 'overstressed' in the baseline period. The mean coverage of stressed areas is expected to remain stable in 2070–2099 under IS, with only a slight increase in 'overstressed' area (15%). In the meantime under HS, the total stressed area is projected to reach 30% with the 'overstressed' coverage expanding to 18% in area and 24% in population.

To identify the hotspot areas with potential increases or decreases in water stress level (Fig. 10), we investigated the spatial distribution of mean multi-decadal changes across the 2099 HUC-8 watersheds and the consensus among results derived from different climate models. Areas expected to endure higher stress levels (i.e., from 'unstressed' to 'upstream-stressed', from 'upstream-stressed' to 'overstressed', or directly from 'unstressed' to 'overstressed') are mainly distributed in the central and western CONUS across WRR#10–17, especially in Missouri (WRR#10), Arkansas-White-Red (WRR#11), Texas-Gulf (WRR#12), Upper Colorado (WRR#14), and Great Basin (WRR#16). Under HS, higher stress level is also projected to occur in a few watersheds in the east. On the other hand, areas shifting to lower stress levels are mostly distributed in the northeast (WRR#2 Mid-Atlantic), the Midwest (WRR#5 Ohio, WRR#7 Upper Mississippi, WRR#10 Missouri), and the southeast (WRR#3 South Atlantic-Gulf, WRR#6 Tennessee).

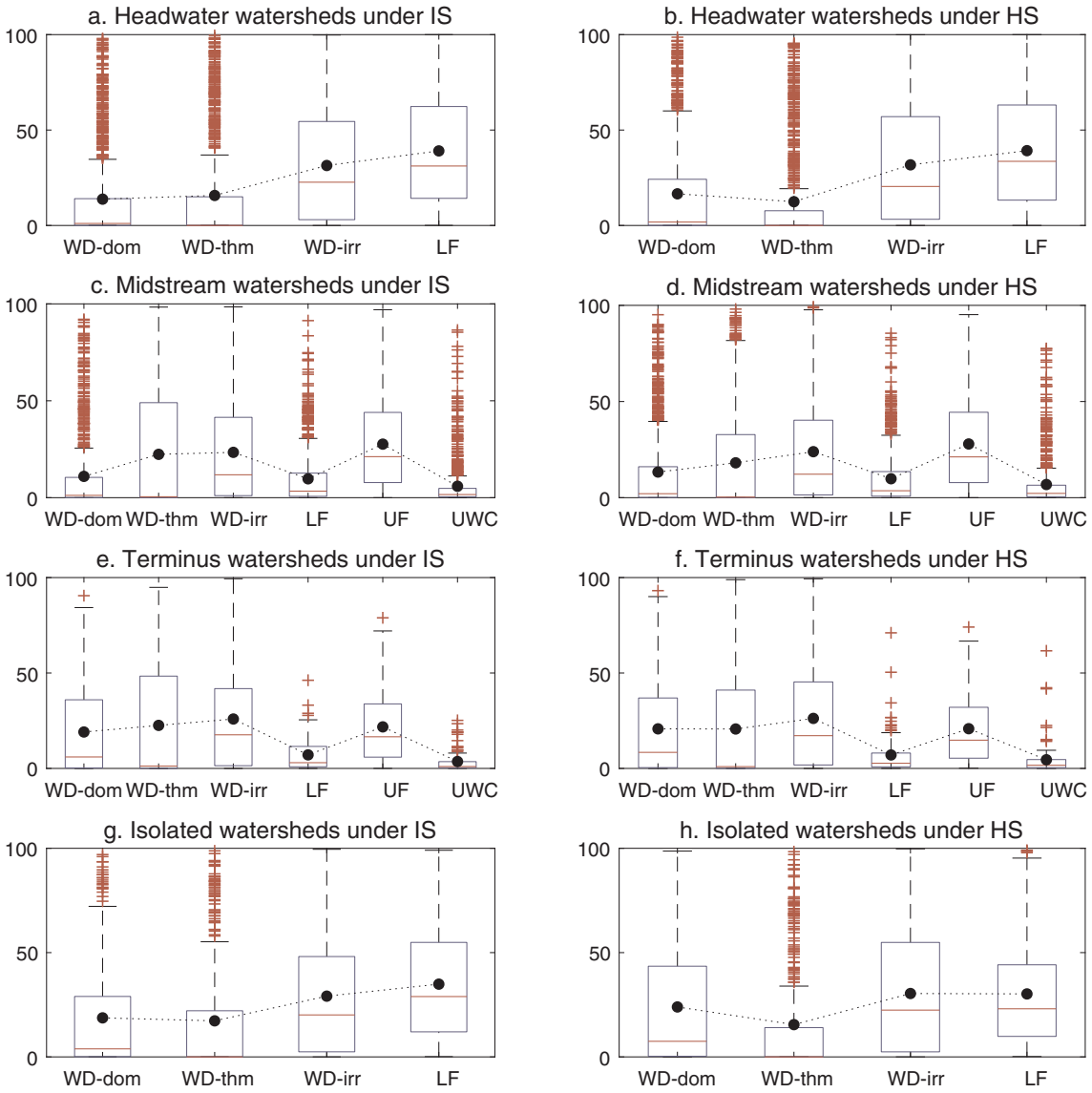

Fig. 8. Attribution (%) of projected changes in water stress in 'headwater' (a–b), 'midstream' (c–d), 'terminus' (e–f), and 'isolated' (g–h) watersheds. The contributors are denoted by WD-dom (domestic water demand), WD-thm (thermoelectric water demand), WD-irr (irrigation water demand), LF (local flow), UF (upstream flow), and UWC (upstream water consumption) on the × axis. The vertical spread of the box–whisker plots shows the variations in relative contribution (%) among watersheds of each type based on multi-model mean projections under the scenarios of Intermediate Stress (IS) and High Stress (HS). The boxes cover the ranges from the 25% quartile to the 75% quartile of the distributions, with the median values marked by red lines within each box and outliers marked by plus signs. The mean contributions of each factor are marked with black circles. (For interpretation of the references to colour in this figure legend, the reader is referred to the web version of this article.)

In total, there are 133 and 192 watersheds facing increased stress levels under the IS and HS scenarios, and high consensus among climate models can be found in 60 and 102 of them, respectively (Table 2). The spatial pattern suggests that 80%–87% of the transitions to 'overstressed' are likely to occur in 'headwater' and 'isolated' watersheds, where water supply is generally more sensitive to climate change due to the limited water source area. Conversely, 'terminus' watersheds are usually endowed with large amounts of upstream water and thus they are more resilient to future changes, with only 4–5 shifts (2–3 with high consensus) between the states of 'unstressed' and 'upstream-stressed' expected. Diverse changes are expected among the 'midstream' watersheds. Although the total number of 'midstream' watersheds facing higher stress is close to that of 'headwater' watersheds, less than half of them are expected to reach the level of 'overstressed', while the rest are increasing from 'unstressed' to 'upstream-stressed'.

The projected future changes will also challenge the efficiency of current IBT projects. The stress escalations in watersheds receiving IBT water (Table 3), particularly for a few 'headwater' and 'isolated' watersheds where only local water is available in the natural state, indicate an increasing need for transferred water in these areas. More shifts to the 'overstressed' status (9–12) are projected in watersheds supplying IBT water. The higher stress levels in these source areas are likely to compromise their capability of providing water and even trigger new conflicts over water rights.

4. Discussion

This study aimed to explore the diverse responses of regional water demand and supply to multiple stressors and provide a reference for water planning and management in a changing world. Our results suggest that previous projections without concern for water connectivity among regions (Devineni et al., 2015; Foti et al., 2012; Roy

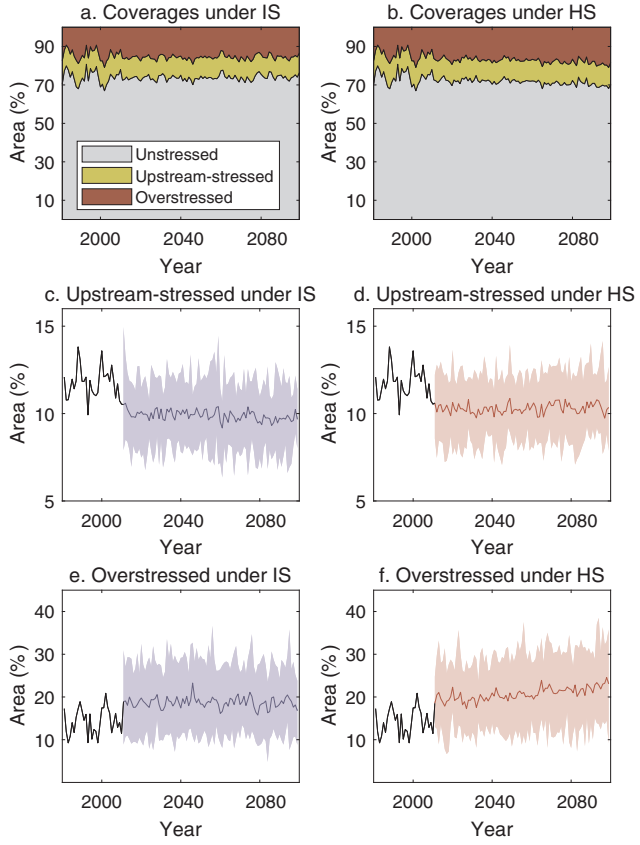

Fig. 9. Temporal variations in the coverages of stressed areas (%) in the CONUS from 1981 to 2099. Multi-model means of the areal coverages of 'unstressed', 'upstream-stressed', and 'overstressed' regions are shown in a–b. The uncertainty ranges derived from multiple climate models are shown for upstream-stressed (c–d) and overstressed (e–f) regions.

et al., 2012) could be misleading. In spite of the spatial differences, water supply in the CONUS is generally more resilient to climate change and increases in water use when non-local water is taken into account. This is not only because of the additional water supplies, but also due to the possibly inhomogeneous changes in runoff generation and water uses in the water source areas. For example, the negative effects of decreasing upstream flow caused by climate change could be partially neutralized or even overwhelmed by the decreasing upstream water uses in some western basins. It is important for water managers to understand that the status of water connectivity among regions are not always stationary over time. Climate change may cause a depletion in upstream water flows and larger evaporation loss during water uses, while the increases in population, energy demand, and irrigation area will impact the quantity and quality of water available for downstream areas. Current legal systems governing water allocation and water rights (e.g., riparian rights in the east and prior appropriation in the west) across the country have been developed based on historical information on water availability and demand. The extensive changes in the future (e.g., depleting river discharge, larger withdrawal demand, lower water level in water intake points) will impose new challenges on the existing systems and the supporting infrastructure. Efficient water management will require a more specific identification of the potential sources of water and an integrated monitoring of their variations and the driving factors (McNulty et al., 2018). This study contributes to our understanding of the critical role of water connectivity to water supply security in the U.S. and can help policy makers and stakeholders to better adapt to the future.

Nevertheless, long-term projections are usually developed under a series of assumptions and thus inevitably involve various uncertainties in the datasets and results. For simplicity the analysis presented in this paper is limited to a few of the most important factors. We here address the uncertainties and limitations inherent to the projections of water demand, consumption, and supplies.

Thermoelectric and irrigation are by far the largest water use sectors, and are also the major sources of uncertainty in the projections of water withdrawal and consumption. We estimated future thermoelectric withdrawal based on historical trends and extrapolation of the EIA's projections. Future shifts in energy policy and technology innovation may cause more complex changes in electricity demand, energy structure, and water use efficiency. For example, renewable energy production such as biofuels (biodiesel and ethanol) is expected to increase as an alternative to thermoelectric power (Elcock, 2010), which could bring in new water requirements for irrigation and exacerbate water stress (Hejazi et al., 2015); carbon capture and storage (CCS) technology is increasingly implemented to curb greenhouse gas emissions from fossil fuel power plants (Rao and Rubin, 2002), and the operation of plants with CCS facility also requires extra water uses. Besides, large uncertainties are involved in the responses of irrigation areas, cropping patterns, and irrigation methods to various climatic, political (e.g., agricultural policies and subsidies), and economic (e.g., agricultural product markets, land prices) forces (Elliott et al., 2014; Wada et al., 2011; Webber et al., 2016). It is still challenging to incorporate all the driving factors and forecast irrigation water demand and consumption rates for a specific time or location.

The projection of water yield and streamflow dynamics is another major source of uncertainty (Milly et al., 2005). Besides the preset assumptions involved in the emission scenarios, structure and parameters of climate model, hydrologic model, and downscaling approach all contribute to the uncertainties to various extents as hydro-climatic simulations are conducted in different contexts or at different spatio-temporal scales (Bae et al., 2011; Bosshard et al., 2013; Duan and Mei, 2014; Giuntoli et al., 2015; Kay et al., 2009). In particular, two caveats should be noted when interpreting our results: (1) Water loss in aqueducts and reservoirs. Water projects including reservoirs, dams, and aqueducts are designed to redistribute water resources spatially and temporally for securing water supply in dry areas or dry seasons. However, a considerable amount of water could be lost in the process through evaporation and leakage. The magnitude of loss depends on many factors including background climate, topography, and river morphology, as well as the design, investment, and maintenance of the infrastructure. More information needs to be collected from local levels to account for the effects of these potential water losses. (2) Interactions between surface water and deep groundwater. In this evaluation, we have focused on surface water while groundwater was excluded from both the demand and supply aspects. However, the enhanced interactions between surface water and groundwater caused by human activities could add to the uncertainty in our results. For example, water loss to deep aquifer storage in the processes of streamflow routing, water transfers, and return flows from irrigation water uses might compromise the availability of upstream water for many downstream areas. In addition, alternative water resources (e.g., saline water, groundwater, rainfall harvest, and reclaimed water) will become more common in the future, and the withdrawals and discharges of these waters could also alter the terrestrial water balance and storage (Döll et al., 2012). In future studies, improved national datasets of water management, especially the consumptive uses and return flows in different sectors and updates of inter-basin transfers, and better representations of the integrated water cycles driven by climate change and human activities are needed to reduce uncertainties.

5. Conclusions

This study demonstrates the potential responses of surface water supply stress to future climatic and socioeconomic changes in the CONUS. By explicitly including watershed-level natural and artificial

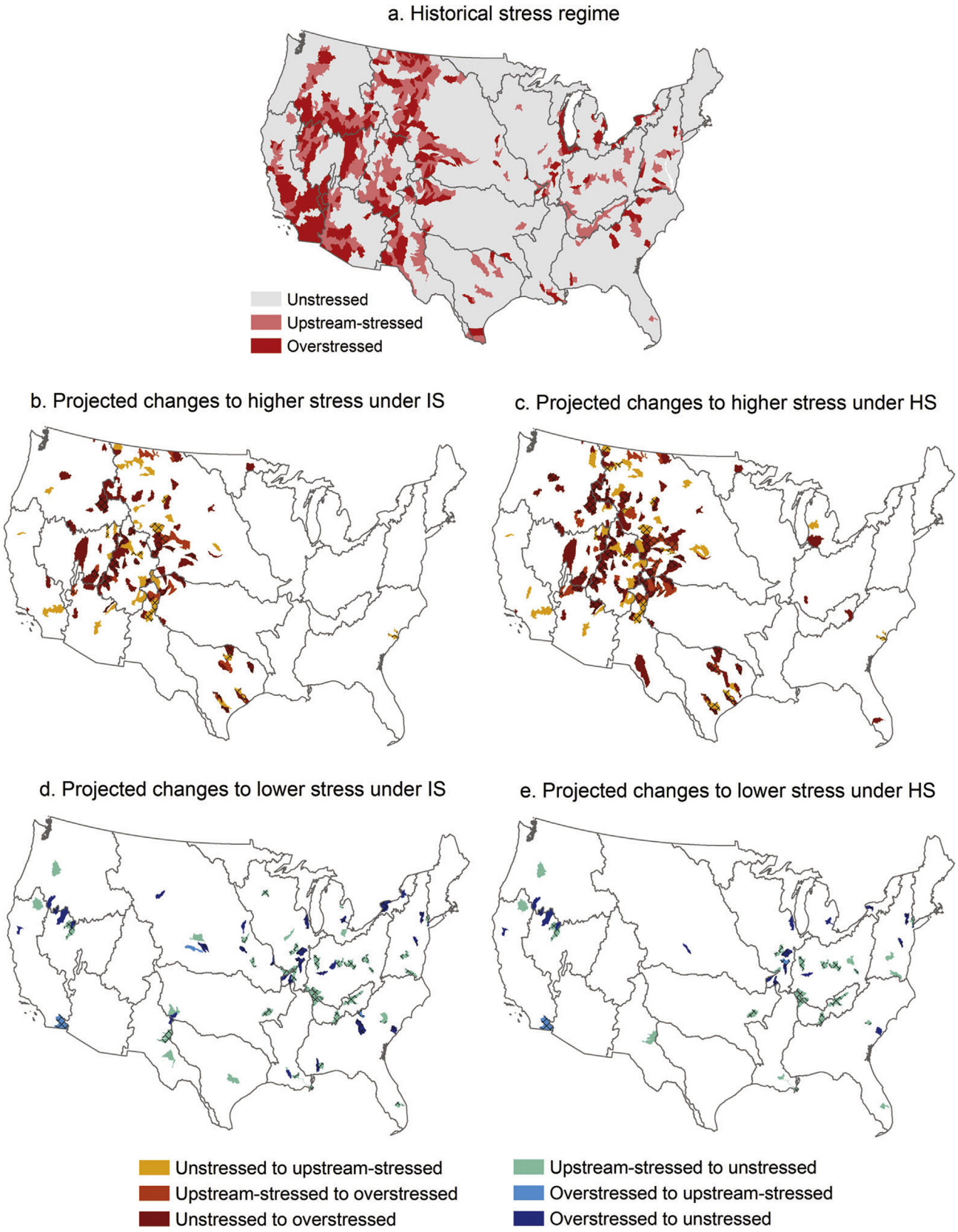

Fig. 10. Historical (1981–2010) and projected changes (2070–2099) in stress regime across the HUC-8 watersheds under the scenarios of Intermediate Stress (IS) and High Stress (HS). The displayed changes in Fig. b–e are based on the ensemble means derived from the climate models, and the watersheds are crosshatched where more than 80% of the models agree on the changing type.

Table 2
Distribution of projected changes in water stress level from historical (1981–2010) to future (2011–2099) scenarios of Intermediate Stress (IS) and High Stress (HS) across the HUC-8 watersheds. The numbers of watersheds shown in the table are derived from the ensemble means of climate models, and the numbers of watersheds where more than 80% of the models agree on the changing sign are marked by brackets.

Change in stress level	IS scenario				HS scenario			
	Headwater	Midstream	Terminus	Isolated	Headwater	Midstream	Terminus	Isolated
Unstressed ↗ Upstream-stressed	3 (0)	27 (11)	4 (2)	2 (1)	0	43 (19)	5 (3)	2 (0)
Upstream-stressed ↗ Overstressed	7 (3)	10 (3)	0	1 (0)	7 (6)	20 (7)	0	2 (0)
Unstressed ↗ Overstressed	50 (25)	10 (3)	0	19 (12)	74 (42)	16 (9)	0	23 (16)
Upstream-stressed ↘ Unstressed	8 (7)	39 (33)	5 (4)	5 (5)	8 (7)	30 (23)	2 (2)	4 (4)
Overstressed ↘ Upstream-stressed	0	1 (1)	1 (1)	0	0	1 (1)	1 (1)	0
Overstressed ↘ Unstressed	16 (9)	1 (1)	0	6 (5)	6 (1)	0	0	5 (2)

Table 3
Same as Table 2, but for watersheds supplying or receiving inter-basin transferred water.

Change in stress level	IS scenario		HS scenario	
	Supplying	Receiving	Supplying	Receiving
Unstressed ↗ Upstream-stressed	4 (1)	7 (2)	6 (2)	7 (2)
Upstream-stressed ↗ Overstressed	1 (0)	0	1 (0)	0
Unstressed ↗ Overstressed	8 (5)	4 (3)	11 (8)	8 (6)
Upstream-stressed ↘ Unstressed	8 (7)	7 (7)	5 (5)	6 (5)
Overstressed ↘ Upstream-stressed	0	1 (1)	0	1 (1)
Overstressed ↘ Unstressed	1 (1)	2 (2)	1 (1)	2 (2)

water connectivity, we explored the distinct roles of water withdrawal, consumptive use, and local and non-local water sources in water supply. In despite of the considerable uncertainty spreads, two main conclusions can be drawn. First, climate change mitigation practices could alleviate water stress from both the aspects of water demand and water supply. The implementation of emission mitigation measures, including the Clean Power Plan program and other socio-economic developments associated with the SRES and RCP scenarios, would lead to a reduction in total water demand by 21% (7.6×10^{10} m^3/yr) and an increase in total water supply by 4% (8.0×10^{10} m^3/yr) (estimated by the multi-model means in 2070–2099). Consequently, the coverage of highly stressed area is expected to remain relatively stable by 2070–2099 with mitigation measures, but to expand from 14% to 18% (from 19% to 24% by population) in a future without mitigation.

Second, water connectivity among watersheds can significantly buffer the impacts of climatic and anthropogenic changes on regional water stress. We show that upstream water and transferred water not only significantly relieved stress in 12% of the CONUS in the historical period, but could also reduce the sensitivity of stress levels to future changes. Spatial patterns suggest that watersheds relying solely on local water resource are more vulnerable to climate change and more likely to face severe stress escalation. Water stress in watersheds receiving water from upstream or from transferred water, can be alleviated by complementary non-local water and also partly be offset by the diverse changes in consumptive uses and water supplies from different source areas. This study raises questions about the potential over or under-estimation of climate change impact on water supply stress where water connectivity among regions is not properly considered. Further studies on the nonstationary role of water connectivity to water supply security and the interactions among multiple environmental and anthropogenic stressors are warranted to better adapt to the changing world.

Declaration of interests

None.

Acknowledgements

This work was supported by the USDA Forest Service Watershed program, the National Key Research and Development Program of China (2017YFC0405900, 2016YFC0401300), the National Natural Science Foundation of China (91547108, 51879289), and the Outstanding Youth Science Foundation of NSFC (51822908).

References

Abatzoglou, J.T., Brown, T.J., 2012. A comparison of statistical downscaling methods suited for wildfire applications. Int. J. Climatol. 32 (5), 772–780.
Alcamo, J., Henrichs, T., Rösch, T., 2000. World water in 2025 – Global modeling and scenario analysis for the World Commission on Water for the 21st Century. Center for Environmental Systems Research, University of Kassel, Kassel, Germany.
Allen, R.G., Pereira, L.S., Raes, D., Smith, M., 1998. Crop evapotranspiration-Guidelines for computing crop water requirements-FAO Irrigation and drainage paper 56. FAO, Rome 300 (9), D05109.
Bae, D.-H., Jung, I.-W., Lettenmaier, D.P., 2011. Hydrologic uncertainties in climate change from IPCC AR4 GCM simulations of the Chungju Basin, Korea. J. Hydrol. 401 (1), 90–105.
Blanc, E., et al., 2014. Modeling US water resources under climate change. Earth's Future 2 (4), 197–224.
Bosshard, T., et al., 2013. Quantifying uncertainty sources in an ensemble of hydrological climate-impact projections. Water Resour. Res. 49 (3), 1523–1536.
Brown, T.C., Foti, R., Ramirez, J.A., 2013. Projected freshwater withdrawals in the United States under a changing climate. Water Resour. Res. 49 (3), 1259–1276.
Caldwell, P., Sun, G., McNulty, S., Cohen, E., Moore Myers, J., 2012. Impacts of impervious cover, water withdrawals, and climate change on river flows in the conterminous US. Hydrol. Earth Syst. Sci. 16 (8), 2839–2857.
Caldwell, P.V., et al., 2015. A comparison of hydrologic models for ecological flows and water availability. Ecohydrology 8 (8), 1525–1546.
Daly, C., et al., 2008. Physiographically sensitive mapping of climatological temperature and precipitation across the conterminous United States. Int. J. Climatol. 28, 2031–2064.
Devineni, N., Lall, U., Etienne, E., Shi, D., Xi, C., 2015. America's water risk: current demand and climate variability. Geophys. Res. Lett. 42 (7), 2285–2293.
Döll, P., 2002. Impact of climate change and variability on irrigation requirements: a global perspective. Clim. Change 54 (3), 269–293.
Döll, P., et al., 2012. Impact of water withdrawals from groundwater and surface water on continental water storage variations. J. Geodyn. 59, 143–156.
Döll, P., et al., 2015. Integrating risks of climate change into water management. Hydrol. Sci. J. 60 (1), 4–13.
Döll, P., Siebert, S., 2002. Global modeling of irrigation water requirements. Water Resour. Res. 38 (4).
Duan, K., Mei, Y., 2014. Comparison of meteorological, hydrological and agricultural drought responses to climate change and uncertainty assessment. Water Resour. Manage. 28 (14), 5039–5054.
Duan, K., et al., 2016. Divergence of ecosystem services in US National Forests and Grasslands under a changing climate. Sci. Rep. 6. https://doi.org/10.1038/srep24441.
Duan, K., et al., 2017a. Impact of air pollution induced climate change on water availability and ecosystem productivity in the conterminous United States. Clim. Change 140 (2), 259–272.
Duan, K., et al., 2017b. Future shift of the relative roles of precipitation and temperature in controlling annual runoff in the conterminous United States. Hydrol. Earth Syst. Sci. 21 (11), 5517–5529. https://doi.org/10.5194/hess-2016-493.
Duan, K., Sun, G., Caldwell, P.V., McNulty, S.G., Zhang, Y., 2018. Implications of upstream flow availability for watershed surface water supply across the conterminous United States. J. Am. Water Resour. Assoc. 54 (3), 694–707. https://doi.org/10.1111/1752-1688.12644.
EIA, 2016. Annual Energy Outlook 2016: with Projections to 2040, Energy Information Administration, US Department of Energy, Washingto, DC.
Elcock, D., 2010. Future US water consumption: The role of energy production. J. Am.

Water Resour. Assoc. 46 (3), 447–460. https://doi.org/10.1111/j.1752-1688.2009.00413.x.
Elliott, J., et al., 2014. Constraints and potentials of future irrigation water availability on agricultural production under climate change. Proc. Natl. Acad. Sci. 111 (9), 3239–3244.
Emanuel, R.E., Buckley, J.J., Caldwell, P.V., McNulty, S.G., Sun, G., 2015. Influence of basin characteristics on the effectiveness and downstream reach of interbasin water transfers: displacing a problem. Environ. Res. Lett. 10 (12), 124005. https://doi.org/10.1088/1748-9326/10/12/124005.
Feeley, T.J., et al., 2008. Water: a critical resource in the thermoelectric power industry. Energy 33 (1), 1–11.
Feng, S., Fu, Q., 2013. Expansion of global drylands under a warming climate. Atmos. Chem. Phys 13 (19), 10081–10094.
Foti, R., Ramirez, J.A., Brown, T.C., 2012. Vulnerability of US water supply to shortage: a technical document supporting the Forest Service 2010 RPA Assessment.
Giuntoli, I., Vidal, J.-P., Prudhomme, C., Hannah, D.M., 2015. Future hydrological extremes: the uncertainty from multiple global climate and global hydrological models. Earth Syst. Dyn. 6 (1), 267–285.
Hejazi, M.I., et al., 2015. 21st century United States emissions mitigation could increase water stress more than the climate change it is mitigating. Proc. Natl. Acad. Sci. 112 (34), 10635–10640.
Hu, Q., et al., 2017. Identifying changes in irrigation return flow with gradually intensified water-saving technology using HYDRUS for regional water resources management. Agric. Water Manag. 194, 33–47.
IPCC, 2014. Climate Change 2014: Synthesis Report. Contribution of Working Groups I, II and III to the Fifth Assessment Report of the Intergovernmental Panel on Climate Change. 9291691437, IPCC, Geneva, Switzerland.
Jackson, R.B., et al., 2005. Trading water for carbon with biological carbon sequestration. Science 310 (5756), 1944–1947.
Kay, A., Davies, H., Bell, V., Jones, R., 2009. Comparison of uncertainty sources for climate change impacts: flood frequency in England. Clim. Change 92 (1–2), 41–63.
Kiguchi, M., Shen, Y., Kanae, S., Oki, T., 2015. Re-evaluation of future water stress due to socio-economic and climate factors under a warming climate. Hydrol. Sci. J. 60 (1), 14–29.
Liu, N., Sun, P., Liu, S., Sun, G., 2013. Coupling simulation of water-carbon processes for catchment calibration and validation of the WaSSI-C model. Chin. J. Plant Ecol. 37 (6), 492–502.
Livneh, B., et al., 2013. A long-term hydrologically based dataset of land surface fluxes and states for the conterminous United States: update and extensions. J. Clim. 26 (23), 9384–9392.
Maupin, M. et al., 2014. Estimated use of water in the United States in 2010.
McNulty, S., Mack, E.C., Sun, G., Caldwell, P., 2016. Hydrologic modeling for water resource assessment in a developing country: The Rwanda case study. In: Lachassagne, P., Lafforgue, M. (Eds.), Forest and the Water Cycle: Quantity, Quality, Management. Cambridge Scholars Publishing, pp. 181–203.
McNulty S.G., et al. 2018. Determinants of the Forest-Water Relationship. In: Forest and Water on a Changing Planet: Vulnerability, Adaptation and Governance Opportunities: A Global Assessment Report (Irena F. Creed and Meine van Noordwijk, eds.). IUFRO World Series Volume 38. p. 61- 78. Vienna.
Milly, P.C., Dunne, K.A., Vecchia, A.V., 2005. Global pattern of trends in streamflow and water availability in a changing climate. Nature 438 (7066), 347–350.
Moore, B.C., Coleman, A.M., Wigmosta, M.S., Skaggs, R.L., Venteris, E.R., 2015. A High Spatiotemporal Assessment of Consumptive Water Use and Water Scarcity in the Conterminous United States. Water Resour. Manage. 29 (14), 5185–5200.
Mooty, W.S., Jeffcoat, H.H., 1986. Inventory of interbasin transfer of water in the Eastern United States. Geological Survey, US, pp. 86–148.
Moss, R.H., et al., 2010. The next generation of scenarios for climate change research and assessment. Nature 463 (7282), 747–756.
NETL, 2011. Estimating freshwater needs to meet future thermoelectric generation requirements: 2011 Update, National Energy Technology Laboratory, US Department of Energy.
Oki, T., et al., 2001. Global assessment of current water resources using total runoff integrating pathways. Hydrol. Sci. J. 46 (6), 983–995.
Petsch Jr, H.E., 1985. Inventory of interbasin transfers of water in the western conterminous United States. Geological Survey, US, pp. 85–166.
Rao, A.B., Rubin, E.S., 2002. A technical, economic, and environmental assessment of amine-based CO2 capture technology for power plant greenhouse gas control. Environ. Sci. Technol. 36 (20), 4467–4475.
Richey, A.S., et al., 2015. Quantifying renewable groundwater stress with GRACE. Water Resour. Res. 51 (7), 5217–5238.
Roy, S.B., et al., 2012. Projecting water withdrawal and supply for future decades in the US under climate change scenarios. Environ. Sci. Technol. 46 (5), 2545–2556.
Sagarika, S., Kalra, A., Ahmad, S., 2014. Evaluating the effect of persistence on long-term trends and analyzing step changes in streamflows of the continental United States. J. Hydrol. 517, 36–53.
Sailor, D.J., 2001. Relating residential and commercial sector electricity loads to climate—evaluating state level sensitivities and vulnerabilities. Energy 26 (7), 645–657.
Sailor, D.J., Pavlova, A., 2003. Air conditioning market saturation and long-term response of residential cooling energy demand to climate change. Energy 28 (9), 941–951.
Scherer, L., Venkatesh, A., Karuppiah, R., Pfister, S., 2015. Large-scale hydrological modeling for calculating water stress indices: implications of improved spatio-temporal resolution, surface-groundwater differentiation, and uncertainty characterization. Environ. Sci. Technol. 49 (8), 4971–4979.
Smith, M., 1992. CROPWAT: A computer program for irrigation planning and management. Food Agric. Org. 126.
Sun, G., et al., 2011. Upscaling key ecosystem functions across the conterminous United States by a water-centric ecosystem model. J. Geophys. Res. 116. https://doi.org/10.1029/2010JG001573.
Sun, G., McNulty, S.G., Moore Myers, J.A., Cohen, E.C., 2008. Impacts of multiple stresses on water demand and supply across the southeastern united states. J. Am. Water Resour. Assoc. 44 (6), 1441–1457.
Sun, S., et al., 2015a. Drought impacts on ecosystem functions of the US National Forests and Grasslands: Part II assessment results and management implications. For. Ecol. Manage. 353, 269–279.
Sun, S., et al., 2015b. Drought impacts on ecosystem functions of the US National Forests and Grasslands: Part I evaluation of a water and carbon balance model. For. Ecol. Manage. 353, 260–268.
Vörösmarty, C.J., Green, P., Salisbury, J., Lammers, R.B., 2000. Global water resources: vulnerability from climate change and population growth. Science 289 (5477), 284–288.
Wada, Y., Van Beek, L., Bierkens, M.F., 2011. Modelling global water stress of the recent past: on the relative importance of trends in water demand and climate variability. Hydrol. Earth Syst. Sci. 15 (12), 3785–3808.
Ward, F.A., Pulido-Velazquez, M., 2008. Water conservation in irrigation can increase water use. Proc. Natl. Acad. Sci. 105 (47), 18215–18220.
Webber, H., et al., 2016. Uncertainty in future irrigation water demand and risk of crop failure for maize in Europe. Environ. Res. Lett. 11 (7), 074007.